# Improved binding between copper and carbon nanotubes in a composite using oxygen-containing functional groups

*Mina Park [a], Byung-Hyun Kim [a], Sanghak Kim [b], Do-Suck Han [b], Gunn Kim [c], Kwang-Ryeol Lee [a],\**

[a] *Computational Science Center, Korea Institute of Science and Technology, P.O. Box 131, Cheongryang, Seoul 130-650, South Korea*
[b] *R&D Division, Hyundai & Kia Co., Euiwang-si, Kyunggi-do 460-30, South Korea*
[c] *Department of Physics, Kyung Hee University, Seoul 130-701, South Korea*

## ARTICLE INFO

## ABSTRACT

The adsorption of Cu on defective carbon nanotubes (CNTs) functionalized with various surface functional groups, including atomic oxygen (–O), hydroxyl (–OH) and carboxyl (–COOH) groups, was investigated by density functional theory calculation. The chemical interaction analysis revealed that the oxygen of the surface functional group can enhance the interaction between the carbon and Cu. The oxygen of the functional group could either promote electron exchange between Cu and carbon atoms, or directly interact with Cu and, thus, played a key role of a glue between the Cu and the CNT surfaces. Among the functional groups investigated, the carboxyl functional group resulted in the largest and most consistent increase in the Cu binding energies on both pristine and defective CNTs. The present calculations support recent experimental work suggesting an important role of interfacial oxygen in the improvement of the mechanical properties of CNT/Cu composites.

## 1. Introduction

Carbon nanotubes (CNTs) and their interactions with transition metals have drawn much attention for their use in metal catalyst systems [1–3], in nanoelectronic devices [4–7] and as reinforcing components of composite materials [8–11]. For such applications, it is essential to understand and control the interactions between CNTs and metals in a systematic manner. For example, to improve the mechanical properties of CNT/metal composites, it is necessary to enhance the interfacial strength between the CNTs and the metal matrix as well as to increase the dispersion uniformity of the CNTs. Without surface treatment, the binding energies between CNTs and metals such as copper, gold, platinum and aluminum are so small that the interfacial slips between the CNTs and the matrix can occur with relatively low external stress

[9,10]. It was also suggested that the performance and the life time of the transition metal catalyst on the CNT support is dependent on the interfacial property between the metals and the CNT surface [12,13].

Many efforts have been made to understand the interaction mechanism of metal atoms at CNT surfaces. Several first principle calculations have reported the binding geometries, the adsorption energies and the electronic structures of various metal atoms interacting with pristine or defective single-walled CNTs [14–20]. However, most CNT applications involve surface treatment processes to promote a uniform dispersion and/or functionalization of the CNT surface, which would decorate the CNT surfaces with various functional groups [21]. It was widely known that the electronic properties of single-walled CNTs, including the local density of states, are sensitive to the chemical environment [22]. Any change in

the intrinsic electronic structure of the surface should influence the chemical properties of the CNTs, which will eventually affect the CNT/metal interface. It is thus imperative to understand the interaction of metals with functionalized CNTs. It was recently reported that Au, Pt, Ti or Rh adsorption behavior on CNT surface is significantly influenced by the oxygen plasma treatment in both theoretical and experimental studies [23–26]. However, the role of oxygen in various configurations of the functional molecule and topological defect of CNT was not thoroughly investigated.

Herein, we theoretically investigated the chemical interaction between Cu and functionalized defective CNT surfaces based on the density functional theory method. We chose Cu as our metal element because Cu is one of the conducting metals that were reported to form very weak bonds with pristine CNTs [14,15]. The effects of the functional elements on the interaction of Cu are expected to be obviously revealed. More motivation for performing these studies came from the experimental results involving CNT/Cu composites. Recently, Cha et al. reported the observation of enhanced mechanical properties of CNT-reinforced Cu composites using a molecular mixing technique [10]. They also observed oxygen atoms at the interface between CNTs and a Cu matrix, and suggested that these oxygen molecules had a positive effect on the interfacial strength [27]. However, the chemical role of the oxygen at the interface was not determined.

We focused on how functional groups including oxygen affect the binding energy of Cu by examining the interaction behavior of a single Cu atom adsorbed on the outer surface of defective CNTs with and without surface functional groups: atomic oxygen (–O), hydroxyl (–OH) and carboxyl (–COOH) groups. The present calculations showed that the interfacial bonding between Cu and CNTs can be significantly improved by the presence of oxygen-containing functional groups on the CNT surface, although the effect of oxygen varies with the topological configuration of the CNTs.

## 2.    Calculation details

Using first principle calculations based on density functional theory, we obtained the energy-minimized structures of pristine or topologically defective CNTs and the equilibrium bind-

ing configuration summarion of the functional groups on them. Then, we examined the binding behavior of Cu on the (functionalized) CNT surfaces. The (6,6) armchair CNTs with 120 carbon atoms and the (6,6) CNTs with a vacancy (119 carbon atoms) were used for our calculations. The binding energies, $E_b$, of Cu on the (functionalized) CNTs were calculated by

$$E_b = \{E_{tot}[(\text{functionalized})\text{CNT} + \text{Cu}] \\ - E_{tot}[(\text{functionalized})\text{CNT}] - E_{tot}[\text{Cu}]\}, \qquad (1)$$

where $E_{tot}$ is the total energy of the system. The binding energies were corrected using the basis set superposition error (BSSE) correction through the counterpoise method with "ghost" atoms [28]. The negative $E_b$ values denote an exothermic binding process.

All geometry optimization calculations of the CNT/Cu complexes were carried out using spin-resolved density functional theory with the SIESTA code [29,30]. We adopted the generalized gradient approximation (GGA) of Perdew, Berke and Ernzerhof (PBE) [31] for the exchange–correlation energy functional and standard norm-conserving pseudopotentials generated according to the procedure of Troullier and Martins to describe the ion–electron interactions [32]. A split-valence double-ζ basis set plus polarization function (DZP) basis set was employed with an energy cutoff of 150 Ry. To simulate one-dimensional infinite nanotubes, periodic boundary conditions were applied along the tube axis (z-direction). In the lateral (x, y) directions, vacuum regions were 6 Å to avoid image-image interactions between neighboring supercells. As per the Monkhorst–Pack scheme of k-points sampling, five k-points were chosen along the tube axis [33]. All atom positions in the supercell were fully relaxed without any constraints using the conjugate-gradient algorithm, and the convergence threshold was set at 0.04 eV/Å for the forces on each atom.

## 3.    Results and discussion

Table 1 summarizes the calculation results of the present work: equilibrium distances of the chemical bonds, the binding energies and the charge transfer of Cu, CNTs and O determined by Mulliken population analysis. As in the previous works, binding of Cu on pristine CNT (P-CNT) was weak with

**Table 1 – Nearest-neighbor distances between Cu and the carbon(s) ($d_{Cu–C}$), the equilibrium Cu–O distance ($d_{Cu–O}$) for the (functionalized) CNTs, the binding energies of the atomic Cu adsorbed on the (functionalized) CNTs ($E_b$), and the calculated charge transfer of Cu ($\Delta Q_{Cu}$), CNTs ($\Delta Q_{CNT}$) and O ($\Delta Q_O$) due to Cu binding as determined by Mulliken population analysis.**

|  | $d_{Cu–C}$ (Å) | $d_{Cu–O}$ (Å) | $E_b$ (eV) | $\Delta Q_{Cu}$ (e) | $\Delta Q_{CNT}$ (e) | $\Delta Q_O$ (e) |
|---|---|---|---|---|---|---|
| P-CNT/Cu | 2.05/2.32 | – | −0.53 | −0.079 | 0.079 | – |
| P-CNT–O/Cu | 2.07/2.15 | 2.43 | −0.73 | −0.128 | 0.105 | 0.023 |
| P-CNT–OH/Cu | 2.02/2.58 | 2.18 | −1.35 | −0.26 | 0.264 | 0.036 |
| P-CNT–COOH/Cu | 2.02/2.39 | 2.06 | −1.37 | −0.33 | 0.285 | 0.056 |
| SW-CNT/Cu | 2.03/2.26 | – | −1.26 | −0.117 | 0.117 | – |
| SW-CNT–O/Cu | 2.08/2.19/2.51 | 1.96 | −2.70 | −0.294 | 0.005 | 0.289 |
| SW-CNT–OH/Cu | 2.02/2.20 | 2.20 | −1.48 | −0.271 | 0.265 | 0.024 |
| SW-CNT–COOH/Cu | 2.00/2.34/2.55 | 1.97 | −1.95 | −0.278 | 0.26 | 0.03 |
| MV-CNT/Cu | 1.86/1.87/1.92 | – | −3.08 | 0.11 | −0.11 |  |
| MV-CNT–O/Cu | 2.12/2.12/2.51 | 2.00 | −1.82 | −0.248 | 0.161 | 0.087 |
| MV-CNT–OH/Cu | 2.10/2.12/2.40 | 2.14 | −1.04 | −0.199 | 0.159 | 0.061 |
| MV-CNT–COOH/Cu | 2.12/2.23/2.44 | 1.97 | −2.15 | −0.232 | 0.186 | 0.113 |

binding energy of −0.53 eV [14,15]. Any defects on the CNT surface significantly enhanced the adsorption of Cu [19,20]. Calculated binding energies are −1.26 eV for Stone–Wales defective CNT (SW-CNT) and −3.08 eV for monovacancy defective CNT (MV-CNT). It is well known that when vacancies are created in CNTs, the three active dangling bonds rearrange to form the pentagon-enneagon structure [5 + 1DB], which leaves one dangling carbon. However, we observed that Cu adsorption at the vacancy site caused a return of its atomic configuration to the original triangular form with Cu in the center. Significant increase in the binding energy on the vacancy site would result from the three strong Cu–C bonds, as can be inferred from the shorter Cu–C distances ranging from 1.86 to 1.92 Å. However, under most experimental conditions, direct adsorption of Cu on the defects is not expected because the high reactivity of the defect will be readily vanished by adsorbing molecules from the ambient atmosphere or during chemical treatment of the CNTs. The oxygen-containing functional groups are usually found after the chemical treatment process that is widely used in CNT applications [21,34].

The binding energy of Cu on the oxygen decorated CNTs increased in both P-CNT (−0.73 from −0.53 eV) and SW-CNT (−2.70 from −1.26 eV), which reveals that the oxygen enhances the binding between Cu and CNTs. However, atomic oxygen at the vacancy has an opposite effect: the binding energy decreased to −1.82 eV, which is 1.26 eV smaller than in the case without oxygen. This contrasting behavior is caused by the passivation of the active dangling bond by the oxygen, as will be discussed later.

The most probable configurations of oxygen-adsorbed CNTs with and without Cu are shown in Fig. 1. At the P-CNT surface, an oxygen atom was attached to the carbon atoms in the circumferential direction [35], as shown in Fig. 1(a). The oxygen adsorption resulted in an *ether* configuration, in which both adjacent carbon atoms were bound to the oxygen where the original C–C bond was broken. Bond lengths of C–O were 1.40 Å, while the distance between the carbons increased to 2.11 Å. The bond angle of the C–O–C linkage was thus 97.4°. When the atomic Cu was attached around the oxygen of the CNT, Cu was bound to both oxygen and the C1 and C2 carbon atoms (see Fig. 1(d)). The *ether* configuration of the C–O–C atomic group was conserved even after the Cu adsorption. More electron transfer occurred to the CNTs from the Cu compared with the case of lacking oxygen: $\Delta Q_{CNT}$ increased from 0.079 to 0.105$e$. However, the direct electron exchange with oxygen was quite limited ($\Delta Q_O$ = 0.023$e$). It can be thus said that the oxygen atom acts as a promoter for the electron exchange between Cu and carbon atoms. Our density of state (DOS) analysis of Fig. 2(a) revealed that increases in the Cu 3$d$ orbital between −4 and −3 eV were likely associated with the O 2$p$ orbital that is located at about −4 eV.

Fig. 1(b) shows that oxygen on the SW-CNT surface bonded to the site above the C2–C3 bond between the two pentagons, and the C–C bond was retained after the oxygen adsorption. Bond lengths of C–O and C–C bonds were 1.45 and 1.49 Å, respectively. The bond angle of the C–O–C linkage was as low as 61.8°. *Ether* groups with no external constraints (such as dimethyl ether) are characterized by a C–O–C bond angle of about 120° and a C–O bond length of about 1.50 Å. Therefore, the oxygen at the SW defect experienced a high level of topological deformation due to the short distance between the carbon atoms. Fig. 1(e) show that one of the two C–O bonds of the highly-distorted *ether* was broken as the Cu atom approached the oxygen-functionalized SW defect. The change in the atomic configuration significantly enhanced the binding energy of Cu from −1.26 to −2.70 eV. This is distinct to the behavior in P-CNT, where the *ether* configuration was conserved after the Cu adsorption. In contrast to the case of P-CNTs, a significant charge transfer occurred between the Cu and the oxygen ($\Delta Q_{Cu}$ = −0.294$e$ and $\Delta Q_O$ = 0.289$e$). A short Cu–O distance (1.96 Å) indicates further that there was a strong interaction between Cu and oxygen. Partial density of state (PDOS) analysis in Fig. 2(b) shows that the upshifted O 2$p$ orbital had extensive overlap with the upshifted Cu 3$d$ orbital near the Fermi level in addition to the C 2$p$ orbital near −2.5 eV. These hybridizations of the O 2$p$ orbital with both Cu and carbon orbitals contribute to the increased binding energy between Cu and the SW-CNT surfaces.

In the case of MV-CNTs, the oxygen atom was attached to the active dangling carbon, C1 of Fig. 1(c). The oxygen thus passivated the active dangling bond in MV-CNTs, reducing the binding energy of Cu. Chemical stabilization of the dangling carbon in MV-CNT is evident when comparing the PDOSs with and without oxygen as shown in Fig. 3. Direct
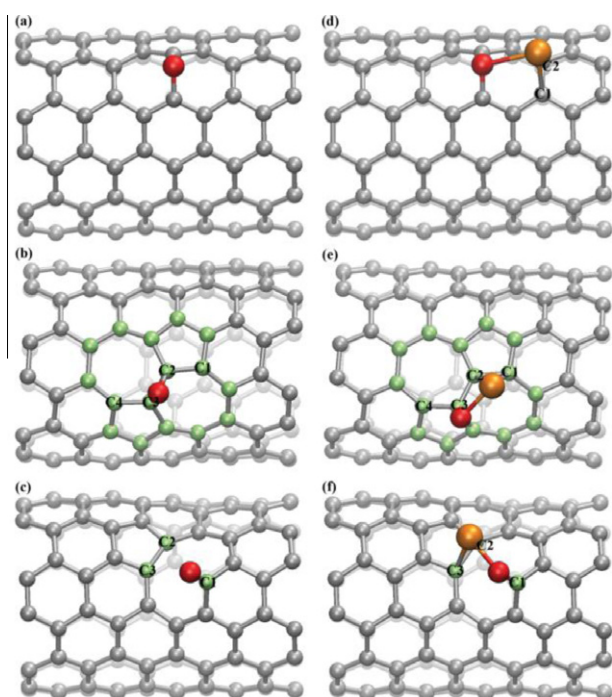


Fig. 1 – Energy minimized structures of the functionalized CNTs with atomic oxygen and their corresponding complex systems with Cu: (a) P-CNT–O, (b) SW-CNT–O, (c) MV-CNT–O, (d) P-CNT–O/Cu, (e) SW-CNT–O/Cu and (f) MV-CNT–O/Cu. The yellow ball represents the Cu atom, green balls represent the carbon atoms composing the defects and the red ball represents the functionalized atomic oxygen. (For interpretation of the references in color in this figure legend, the reader is referred to the web version of this article.)
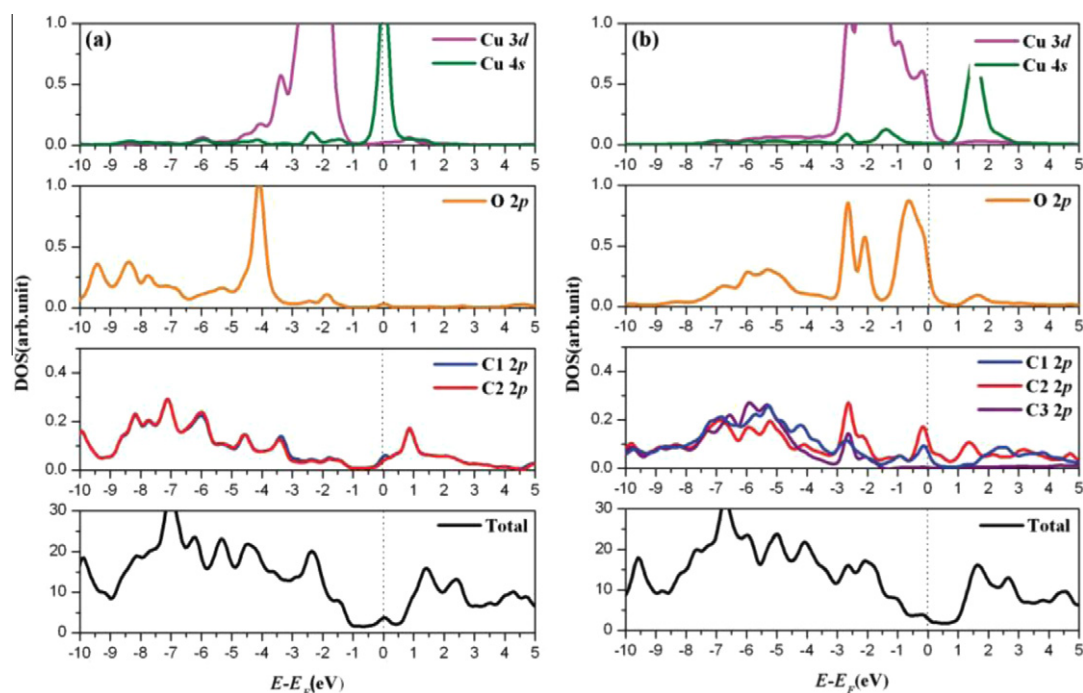
Fig. 2 – Density of states for (a) P-CNT–O/Cu, and (b) SW-CNT–O/Cu. The carbon atom indices correspond to those in Fig. 1.
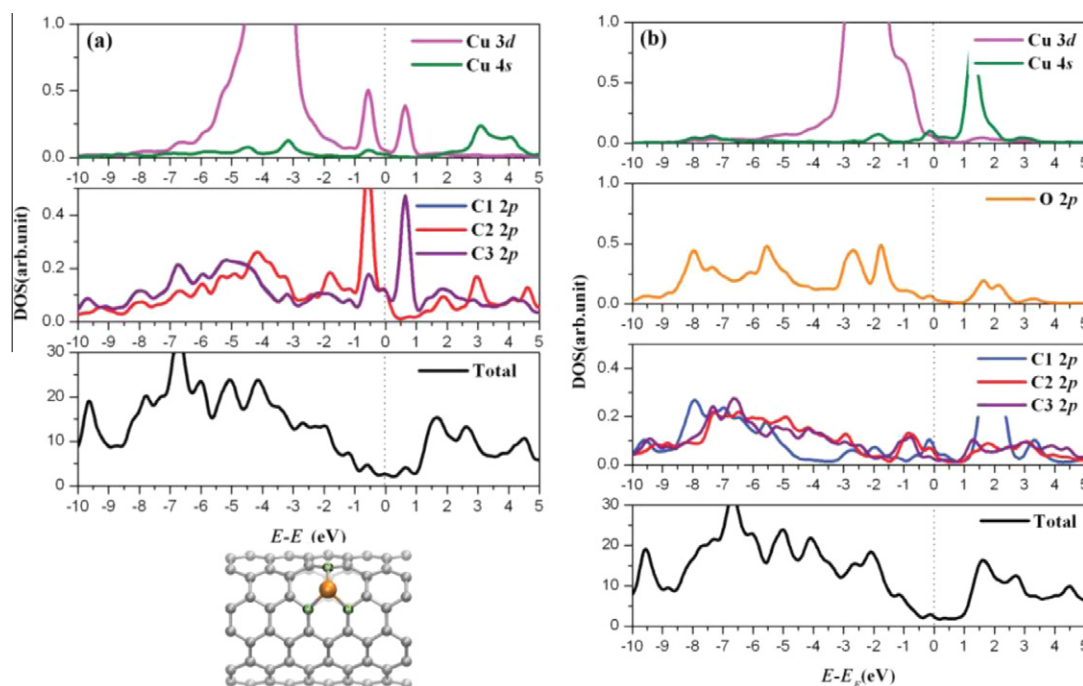


Fig. 3 – Density of states for (a) MV-CNT/Cu, and (b) MV-CNT–O/Cu. The carbon atom indices in (a) correspond to the carbon atoms in the configuration below. The yellow ball represents the Cu atom, green balls represent the carbon atoms composing the vacancy. The carbon atom indices in (b) correspond to those in Fig. 1(f). (For interpretation of the references to colour in this figure legend, the reader is referred to the web version of this article.)

overlap between the orbitals of the Cu and the carbon atoms of vacancy (as shown in Fig. 3(a)) was not observed in the oxygen-functionalized vacancy even though the simultaneous hybridization of oxygen with the orbitals of the Cu and the carbon atoms occurs as it does in the SW defect case (see Fig. 3(b)). The change in the charge of Cu ($\Delta Q_{Cu} = -0.248e$) was slightly smaller than the change observed in the SW-CNT case ($\Delta Q_{Cu} = 0.294e$). Because of a large difference in

the atomic configurations, it was difficult to compare the charge transfer behavior directly with that of the MV-CNTs without oxygen.

Oxygen in the hydroxyl (-OH) functional groups was bound to only one carbon atom in all of the CNTs as shown in Fig. 4(a–c). However, oxygen in hydroxyl functional group exhibits a reduced chemical activity compared with atomic oxygen due to an electron deprivation by the hydrogen. The binding energy of Cu with hydroxyl group was smaller than that with atomic oxygen of the same topological configuration. For example, on both SW-CNTs and MV-CNTs where the atomic oxygen was bound to only one carbon atom in the CNT-Cu complexes, hydroxyl group functionalization decreased the binding energy of Cu from −2.70 to −1.48 eV for the Stone–Wales defect and from −1.82 to −1.04 eV for the monovacancy defect (see Table 1). Reduced activity of oxygen was also confirmed by the DOS analysis and the charge transfer calculation results. The DOS analysis in Fig. 5(b) and (c) show that the PDOS of the O $2p$ orbital near the Fermi level is significantly reduced compared with the PDOS in the atomic oxygen case (see Fig. 2(b) and Fig. 3(b)). Furthermore, the Cu $3d$ and $4s$ orbitals were not significantly shifted by hydroxyl group functionalization. The values of $\Delta Q_{Cu}$ for the hydroxyl



**Fig. 4 – Energy minimized structures of the functionalized CNTs with hydroxyl groups and their corresponding complex systems with Cu: (a) P-CNT–OH, (b) SW-CNT–OH, (c) MV-CNT–OH, (d) P-CNT–OH/Cu, (e) SW-CNT–OH/Cu and (f) MV-CNT–OH/Cu. The yellow ball represents the Cu atom, the green balls represent the carbon atoms composing the defects and the red and blue balls represent the oxygen and hydrogen in the hydroxyl functional groups, respectively. (For interpretation of the references to colour in this figure legend, the reader is referred to the web version of this article.)**
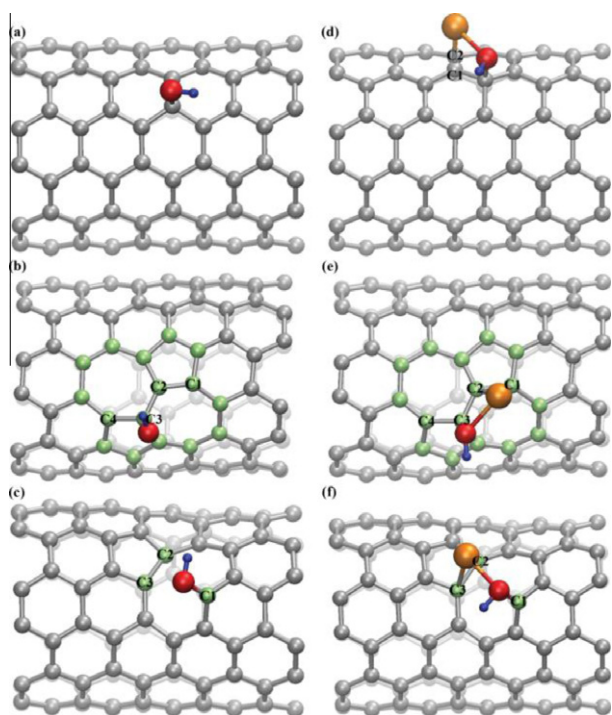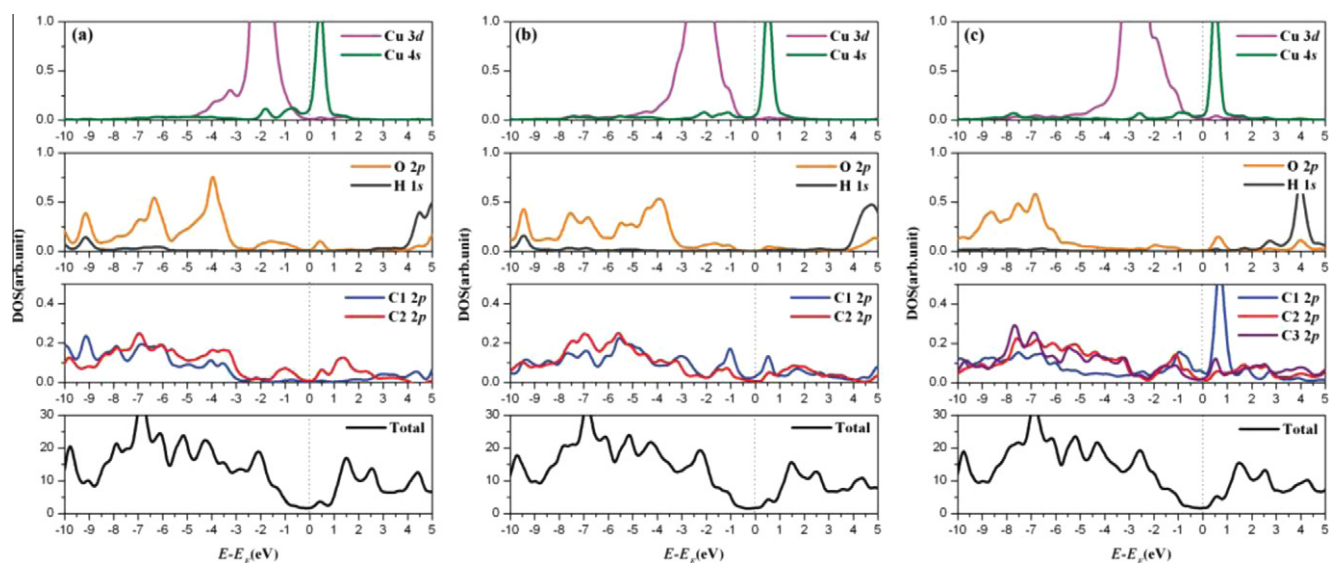
functionalized SW-CNTs or MV-CNTs were also smaller than those for atomic oxygen functionalization (see Table 1).

In contrast to the defective CNTs, the binding energy of Cu on P-CNTs functionalized by hydroxyl group (−1.35 eV) was larger than that for atomic oxygen functionalization (−0.73 eV). This behavior is due to the difference in the atomic configuration of the functionalized CNT wall. In the hydroxyl case, where the hydroxyl molecule binds to only one carbon atom (see Fig. 4(a)), the oxygen is easier to accommodate the Cu adsorption than the atomic oxygen case in which the oxygen forms a stable *ether* (C–O–C) configuration (see Fig. 1(d)). The increased PDOS of the O $2p$ orbital that overlaps with the Cu $3d$ and C $2p$ orbitals (Fig. 5(a)) is in accordance with the increased activity of the oxygen in the hydroxyl functional group interacting with P-CNTs. Table 1 also shows that the $\Delta Q_{Cu}$ (−0.26$e$) was about twice as large as the $\Delta Q_{Cu}$ for the atomic oxygen functionalization case (−0.128$e$).

The change in Mulliken charge population in Table 1 also shows that the ionic bond characteristic in the Cu adsorption increased as the CNT surface is functionalized by the oxygen containing molecules. This result is consistent with the previous experimental analysis of Cu ion adsorption on oxygen decorated activated carbon in aqueous solution [36]. It was suggested that the reaction between Cu and oxygen decorated activated carbon can be described by the surface ionization and ion-exchange mechanism. The changes in Mulliken charge population also revealed that the oxygen on the CNT surface enhanced the surface ionization.

From the atomic oxygen and hydroxyl functional group cases, it can be suggested that functionalization that maintains the chemical activity of the oxygen atom enhances the binding between the CNTs and Cu. It would be thus interesting to examine the effect of carboxyl functional group (–COOH), because the oxygen on the carbonyl side (–C=O) of carboxyl can actively participate in the interaction with Cu regardless to the topological configuration of the CNTs. It is further noted that the CNT surface is frequently functionalized by a carboxyl group during pretreatment processes that use strong acids or other oxidizing agents [37,38].

The carboxyl molecules interact with CNTs in the similar way to the hydroxyl group case: carbon in the carboxyl functional groups was bound to one carbon atom in all pristine and defective CNTs. Similar interaction behaviors of the carboxyl group with carbon were reported in graphene and other CNT systems [39–42]. The adsorbed Cu atom interacted with the oxygen on the carbonyl (–C=O) side of the carboxyl group on the CNT surface. As an example, Fig. 6(a) shows the equilibrium configuration when Cu adsorbed on the COOH decorated MV-CNT. The oxygen in carbonyl side, O1, accumulated electrons by the Cu adsorption (see Table 1). The Cu–O distances for all pristine and defective CNTs were approximately 2.0 Å. Binding energies with Cu were calculated to be −1.37, −1.95 and −2.15 eV for P-CNTs, SW-CNTs and MV-CNTs, respectively. The DOS analysis demonstrate that the PDOSs of the carboxyl group and the nearest neighbor carbon atoms were upshifted toward the Fermi level in the defective CNTs, which enlarged the overlap with the Cu $3d$ orbital (see Fig. 6(b) as an example). It is also evident in Table 1 that the electron exchange between the Cu and carbon atoms was enhanced by the carboxyl group of the CNTs.

Fig. 5 – Density of states for (a) P-CNT–OH/Cu, (b) SW-CNT–OH/Cu and (c) MV-CNT–OH/Cu. The indices of the carbon atoms correspond to those in Fig. 4.
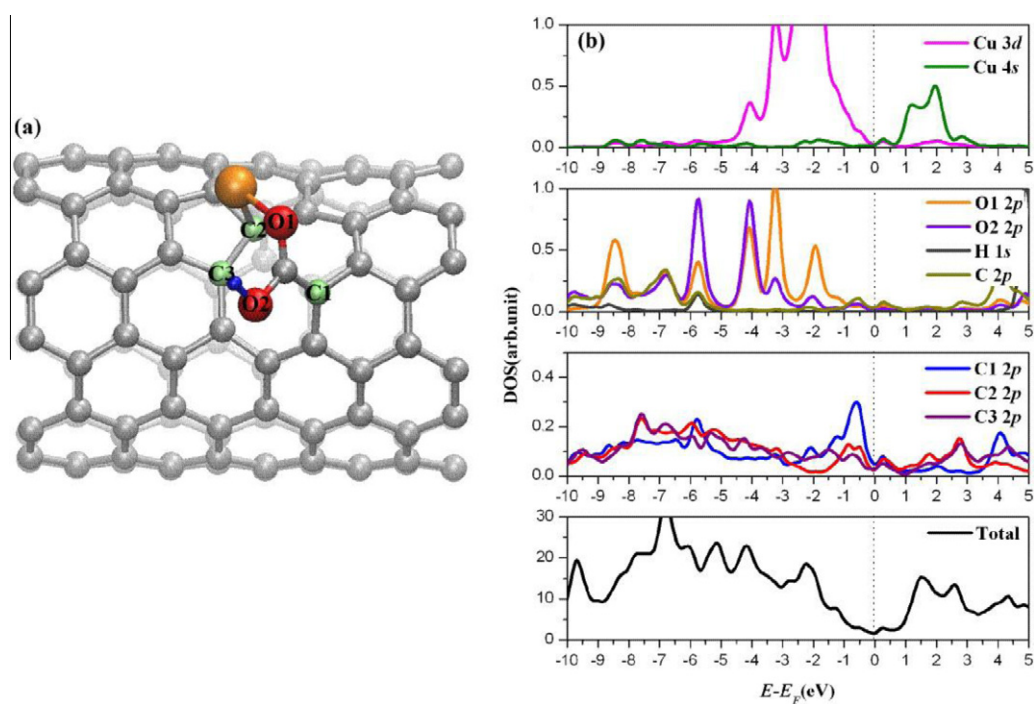


Fig. 6 – (a) Energy minimized structure of Cu and *carboxyl* functionalized MV-CNT complex. The yellow ball represents the Cu atom, the green balls represent the carbon atoms composing the vacnacy, and the red and blue balls represent the oxygen and hydrogen atoms in the *carboxyl* functional group, respectively. (b) Density of states for MV-CNT–COOH/Cu complex. The carbon and oxygen indices correspond to those in (a).

This calculation with carboxyl functionalization group demonstrated the importance of the chemically active oxygen in the binding of Cu on CNT. The significant contribution of the oxygen to the binding of Cu on CNT surface would be also revealed in Fig. 7, which shows that the binding energies of Cu for all three functional groups are inversely proportional to the bond length between Cu and O. The present work suggests that the binding of Cu is dominated by the chemical

interaction with oxygen on the CNT surfaces, while the topological configuration of CNTs can vary the role of oxygen in the chemical reaction. This result is consistent with previous experimental observations which suggested that the mechanical property of CNT-reinforced Cu composite is enhanced by the interfacial oxygen atoms [27].

The present calculation has an important implication for the development of CNT/metal systems including CNT/Cu
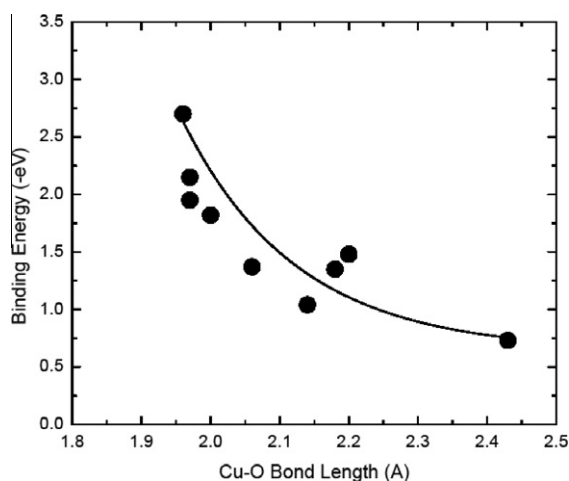
**Fig. 7 – Change of the binding energy of Cu on CNTs for various values of the bond length between Cu and O. Solid line is for guiding the view.**

composites. CNTs used in the experimental processes may have various kinds of defect ranging from vacancy, Stone–Wales defects to unbound carbon edges. The result in Table 1 showed that hydroxyl and carboxyl group functionalization resulted in a consistent enhancement of the binding energy of Cu regardless of the defects in CNTs. On the other hand, atomic oxygen resulted in a large variation of binding energies depending on the defect of CNT. The consistency in the binding energy enhancement would be crucial for the applications of CNT/metal system where the property variation has to be firmly controlled. Since the carboxyl molecule resulted in higher binding energies of Cu than hydroxyl molecule, it would be suggested that the carboxyl molecule is preferable for the surface functionalization for mechanical applications.

## 4.    Conclusion

The binding energies and electronic structures of various CNT/Cu complexes composed of Cu and defective CNTs functionalized with atomic oxygen, hydroxyl groups and carboxyl groups were investigated by density functional theory method. Our calculations showed that the chemically active oxygen in the functionalized CNT surfaces can enhance the binding of Cu with CNTs by promoting the electron exchange between Cu and carbon atoms or directly interacting with Cu. These results support the experimental study that suggested an important role of the oxygen at the interface between a Cu matrix and CNTs [27]. Among the three functionalization groups examined, the carboxyl group was the most optimized molecule with respect to the consistency of the binding energy enhancement of Cu with both pristine and defective CNT surfaces.

## Acknowledgements

REFERENCES

[1] Planeix JM, Coustel N, Coq B, Brotons V, Kumbhar PS, Dutartre R, et al. Application of carbon nanotubes as supports in heterogeneous catalysis. J Am Chem Soc 1994;116(17):7935–6.
[2] Serp P, Corrias M, Kalck P. Carbon nanotubes and nanofibers in catalysis. Appl Catal A 2003;253(2):337–58.
[3] Peng F, Zhang L, Wang H, Lv P, Yu H. Sulfonated carbon nanotubes as a strong protonic acid catalyst. Carbon 2005;43(11):2405–8.
[4] Tans SJ, Verschueren RM, Dekker C. Room-temperature transistor based on a single carbon nanotube. Nature 1998;393:49–52.
[5] Inoue S, Matsumura Y. Molecular dynamics simulation of physical vapor deposition of metals onto a vertically aligned sing-walled carbon nanotube surface. Carbon 2008;46(15):2046–52.
[6] Deng WQ, Matsuda Y, Goddard III WA. Bifunctional anchors connecting carbon nanotubes to metal electrodes for improved nanoelectronics. J Am Chem Soc 2007;129(32):9834–5.
[7] Matsuda Y, Deng WQ, Goddard III WA. Improving contact resistance at the nanotube–Cu electrode interface using molecular anchors. J Phys Chem C 2008;112(29):11042–9.
[8] Ajayan PM, Tour JM. Nanotube composites. Nature 2007;447:1066–8.
[9] Kwon H, Estili M, Takagi K, Miyazaki T, Kawasaki A. Combination of hot extrusion and spark plasma sintering for producing carbon nanotube reinforced aluminum matrix composites. Carbon 2009;47(3):570–7.
[10] Cha SI, Kim KT, Arshad SN, Mo CB, Hong SH. Extraordinary strengthening effect of carbon nanotubes in metal-matrix nanocomposite processed by molecular-level mixing. Adv Mater 2005;17(11):1377–81.
[11] Diez-Pascual AM, Naffakh M, Gomez MA, Marco C, Ellis G, Teresa Martinez M, et al. Development and characterization of PEEK/carbon nanotube composites. Carbon 2009;47(13):3079–90.
[12] Hsin YL, Hwang KC, Yeh CT. Poly(vinylpyrrolidone)-modified graphite carbon nanofibers as promising supports for PtRu catalysts in direct methanol fuel cells. J Am Chem Soc 2007;129(32):9999–10010.
[13] Zhang J, Liu X, Blume R, Zhang A, Schlögl R, Su DS. Surface-modified carbon nanotubes catalyze oxidative dehydrogenation of n-butane. Science 2008;322:73–7.
[14] Durgun E, Dag S, Bagci VMK, Gűlseren O, Yildirim T, Ciraci S. Systematic study of adsorption of single atoms on a carbon nanotube. Phys Rev B 2003;67. R201401-1–4.
[15] Durgun E, Dag S, Ciraci S, Gűlseren O. Energetic and electronic structures of individual atoms adsorbed on carbon nanoutbes. J Phys Chem B 2004;108(2):575–82.
[16] Park N, Sung D, Lim S, Moon S, Hong S. Realistic adsorption geometries and binding affinities of metal nanoparticles onto the surface of carbon nanotubes. Appl Phys Lett 2009;94:073105-1–3.
[17] Yang SH, Shin WH, Kang JK. Ni adsorption on Stone–Wales defect sites in single-wall carbon nanotubes. J Chem Phys 2006;125:084705-1–5.

[18] Johll H, Kang HC, Tok ES. Density functional theory study of Fe, Co, and Ni adatoms and dimers adsorbed on graphene. Phys Rev B 2009;79:245416-1–18.

[19] Zhuang HL, Zheng GP, Soh AK. Interaction between transition metals and defective carbon nanotubes. Comput Mater Sci 2008;43(4):823–8.

[20] Zheng GP, Zhuang HL. Enhanced mechanical strength and ductility of metal-repaired defective carbon nanotubes: a density functional study. Appl Phys Lett 2008;92: 191902-1–3.

[21] Burghard M, Balasubramanian K. Chemically functionalized carbon nanotubes. Small 2005;1(2):180–92.

[22] Collins PG, Bradley K, Ishigami M, Zettl A. Extreme oxygen sensitivity of electronic properties of carbon nanotubes. Science 2000;287:1801–4.

[23] Suarez-Martinez I, Bittencourt C, Ke X, Felten A, Pireaux JJ, Ghijsen J, et al. Probing the interaction between gold nanoparticles and oxygen functionalized carbon nanotubes. Carbon 2009;47(6):1549–54.

[24] Zhang S, Shao Y, Yin G, Lin Y. Carbon nanotubes decorated with Pt nanoparticles via electrostatic self-assembly: a highly active oxygen reduction electrocatalyst. J Mater Chem 2010;20(14):2826–30.

[25] Felten A, Suarez-Martinez I, Ke X, Van Tendeloo G, Ghijsen J, Pireaux JJ, et al. The role of oxygen at the interface between titanium and carbon nanotubes. ChemPhysChem 2009;10:1799–804.

[26] Suarez-Martinez I, Ewels C, Ke X, Van Tendeloo G, Thiess S, Drube W, et al. Study of the interface between rhodium and carbon nanotubes. ACSNano 2010;4(3):1680–6.

[27] Kim KT, Cha SI, Gemming T, Eckert J, Hong SH. The role of interfacial oxygen atoms in the enhanced mechanical properties of carbon-nanotube-reinforced metal matrix nanocomposites. Small 2008;4(11):1936–40.

[28] Boys SF, Bernardi F. The calculation of small molecular interactions by the differences of separate total energies – some procedures with reduced errors. Mol Phys 1970;19(4):553–66.

[29] Ordejón P, Artacho E, Soler JM. Self-consistent order-N density functional calculations for very large systems. Phys Rev B 1996;53(16):10441–4.

[30] Soler JM, Artacho E, Gale JD, García A, Junquera J, Ordejón P, et al. The SIESTA method for *ab initio* order-N materials simulation. J Phys: Condens Matter 2002;14(11):2745–79.

[31] Perdew JP, Burke K, Ernzerhof M. Generalized gradient approximation made simple. Phys Rev Lett 1996;77(18):3865–8.

[32] Troullier N, Martins J. Efficient pseudopotentials for plane-wave calculations. Phys Rev B 1991;43(3):1993–2006.

[33] Monkhorst HJ, Pack JD. Special points for Brillouin-zone integrations. Phys Rev B 1976;13(12):5188–92.

[34] Zhang J, Zou HL, Qing Q, Yang YL, Li QW, Liu ZF, et al. Effect of chemical oxidation on the structure of single-walled carbon nanotubes. J Phys Chem B 2003;107(16):3712–8.

[35] Ashraf MK, Bruque NA, Pandey RR, Collins PG, Lake RK. Effect of localized oxygen functionalization on the conductance of metallic carbon nanotubes. Phys Rev B 2009;79(11):115428.

[36] Biniak S, Pakula M, Szymanski G, Swiatkowski A. Effect of activated carbon surface oxygen- and/or nitrogen-containing groups on adsorption of copper(II) ions from aqueous solution. Langmuir 1999;15:6117–22.

[37] Liu J, Rinzler AG, Dai H, Hafner JH, Bradly RK, Boul PJ, et al. Fullerene pipes. Science 1998;280:1253–6.

[38] Zhao W, Song C, Pehrsson PE. Water-soluble and optically pH-sensitive single-walled carbon nanotubes from surface modification. J Am Chem Soc 2002;124(49):12418–9.

[39] Zhao J, Park H, Han J, Lu JP. Electronic properties of carbon nanotubes with covalent sidewall functionalization. J Phys Chem B 2004;108(14):4227–30.

[40] Wang C, Zhou G, Liu H, Wu J, Qiu Y, Gu B, et al. Chemical functionalization of carbon nanotubes by carboxyl groups on Stone–Wales defects: a density functional theory study. J Phys Chem B 2006;110(21):10266–71.

[41] Li Y, Zhou Z, Golberg D, Bando Y, Ragué Schleyer P, Chen Z. Stone–Wales defects in single-walled boron nitride nanotubes: formation energies, electronic structures, and reactivity. J Phys Chem C 2008;112(5):1365–70.

[42] Wang C, Zhou G, Wu J, Gu B, Duan W. Effects of vacancy–carboxyl pair functionalization on electronic properties of carbon nanotubes. Appl Phys Lett 2006;89:173130-1–3.